

## Induced staggered magnetic fields in antiferromagnets: Microscopic mechanisms

N. Giordano\* and W. P. Wolf

*Department of Engineering and Applied Science, Becton Center, Yale University, New Haven, Connecticut 06520*

(Received 5 July 1979)

The induced staggered magnetic field effects recently proposed by Blume *et al.* on the basis of general symmetry considerations are discussed in terms of detailed microscopic mechanisms, with special reference to the experimental situation in dysprosium aluminum garnet (DAG). It is shown that all of the low-field effects observed in DAG can be accounted for quantitatively by a mechanism based on the way in which the competing interactions affect the spin-spin correlations. Approximate calculations of the high-field effects are also discussed, and it is found that the same mechanism is probably responsible for these as well. A second mechanism, which is based upon the inequivalence of the  $g$  tensors of different spins is also considered, and although this mechanism does not appear to be important in any of the experiments performed to date, we find that it will be the dominant mechanism at both low and high temperatures. It is possible for the two mechanisms to compete, and if this should be the case, it would lead to a new phase transition in a hitherto uninvestigated region of the phase diagram below about 1.1 K. Two additional mechanisms involving higher-order Zeeman effects and anisotropic non-Ising spin-spin interactions are also considered, but their effects are found to be negligible in DAG. In other antiferromagnets for which symmetry also allows induced staggered field effects, any or all of these microscopic mechanisms may be important, and a correspondingly wide range of behavior may be expected. Semiquantitative estimates predict relatively small effects in  $\text{CoF}_2$  and  $\text{FeF}_2$ , but large and readily observable effects in several rare-earth gallium and aluminum garnets.

### I. INTRODUCTION

Dysprosium aluminum garnet (DAG) has been the subject of a large number of experimental studies.<sup>1-3</sup> One reason for the interest in DAG is that it has been found to be a close approximation to an Ising antiferromagnet,<sup>1</sup> and it was therefore considered to be an ideal system in which to study various types of phase transitions. For a time, there was a rather puzzling situation in which some experimental results agreed very well with the usual theoretical predictions, while others, particularly those involving magnetic fields applied along a [111] direction, did not.<sup>1,2,4,5</sup>

The first insight into the solution of this problem was provided by Blume *et al.*,<sup>6</sup> who recognized that DAG belongs to a hitherto unrecognized class of antiferromagnets in which the antiferromagnetic order parameter (the staggered magnetization  $M_s$ ) can couple directly to an applied magnetic field. The idea was extended by Alben *et al.*<sup>7</sup> who considered the general problem from a group-theoretical point of view, and showed that in certain systems it is possible to have terms in the magnetic free energy which are not usually considered, involving  $M_s$  and various third- or higher-order functions of the field. The simplest term of this kind which is allowed in the

case of DAG has the form

$$\Delta F = aH_x H_y H_z M_s, \quad (1)$$

where  $a$  is in general a function of temperature and  $H_x$ ,  $H_y$ , and  $H_z$  are the components of the applied magnetic field. The effect of a term of this kind will be the same as that of a real staggered magnetic field which, if it could be produced in the laboratory, would add a term to the free energy of the form  $\Delta F = -H_s M_s$ . The quantity  $(-aH_x H_y H_z)$  was therefore referred to as an "induced staggered field."<sup>8</sup>

The physical consequences of an induced staggered field were discussed by Blume *et al.*<sup>6</sup> and by Alben *et al.*,<sup>7</sup> who showed that it qualitatively explained a number of the previously puzzling features in the behavior of DAG. In particular, it explains the observed magnetic hysteresis at low temperatures<sup>5,9</sup> which is found to result from an inequivalence of the two time-reversed antiferromagnetic states  $A^+$  and  $A^-$  in the presence of a magnetic field along [111]. It also explains the absence of a second-order phase transition in the presence of a [111] field and the nonsingular variation of the order parameter with field, as observed by neutron scattering.<sup>6</sup>

As in the case of all arguments based on symmetry considerations alone, these explanations did not provide an answer to the physical origin of the mecha-

nism(s) responsible for the induced-staggered-field effects. In the original paper, Blume *et al.*<sup>6</sup> mentioned two possible mechanisms, one involving the inequivalence of the  $g$  tensors at different rare-earth sites, the other involving the anisotropy of the Van Vleck susceptibility. Of these, the  $g$  tensor mechanism was subsequently considered by Foglio and Blume,<sup>10</sup> who concluded that it was too small to account for any of the effects observed in DAG while, as we will see below, the Van Vleck susceptibility mechanism turns out to be ineffective for the particular induced staggered fields which we seek to explain.

In this paper we shall consider two additional mechanisms based on the detailed form of the spin-spin interactions corresponding to the symmetry of the garnet lattice. One of these, involving non-Ising terms in the interactions, is also found to be too weak to account for the behavior observed in DAG, but the other, which depends on the relative *signs* of the Ising-like interactions, is shown to account quantitatively for the principal observations. This mechanism, which we term the *staggered interaction mechanism*, is of particular interest since it results from multiple-spin correlation effects involving three or more spins, which are completely ignored by mean-field and similar approximations.

The relatively subtle nature of the effect which we seek to explain can be appreciated by estimating the size of the induced staggered field which is required to account for the experimental observations. Thus, for example, in the optical magnetization measurements, Dillon *et al.*<sup>9</sup> found a difference in the magnetization  $\Delta M$  between the  $A^+$  and  $A^-$  states amounting to only about 2.5 emu/cm<sup>3</sup> in an applied field of 3.0 kOe and at a temperature of 1.3 K. If we ascribe all of this to a term in the free energy of the form of Eq. (1), we obtain

$$\begin{aligned} \Delta M &= \frac{-\partial[\Delta F(A^+) - \Delta F(A^-)]}{\partial H} \\ &= -2 \frac{aH^2}{\sqrt{3}} M_s = \frac{6H_s}{H} M_s, \end{aligned} \quad (2)$$

where we have put  $H_x = H_y = H_z = H/\sqrt{3}$  corresponding to a [111] field and have identified  $H_s = -aH_x H_y H_z$ . A value for  $|M_s| \sim 600$  emu/cm<sup>3</sup> may be estimated from the neutron scattering results of Blume *et al.*<sup>6</sup> and, solving for  $H_s$ , we obtain  $H_s \sim 2$  Oe. This is less than 0.1% of the applied field, and it is clear that a rather careful approximation may be required to account for the effects properly.

Fortunately, in the case of DAG the microscopic Hamiltonian describing the interactions of the spins with each other and with the field is well known from previous work, and we can therefore start from a rather reliable model for detailed calculations. In Sec.

II we summarize the features of the microscopic structure and interactions which we shall need for our analysis. For the statistical approximations, we shall use series expansions at low and high temperatures, and these will be discussed in Secs. III and IV. A less precise, but for our purposes quite adequate, cluster calculation suitable for intermediate temperatures will be discussed in Sec. V. Quantitative comparisons with the available experimental data are made in the corresponding sections. In Sec. VI we discuss the possible role of various microscopic mechanisms in producing observable induced-staggered-field effects in materials other than DAG, and in Sec. VII we summarize our conclusions which suggest a number of directions which may warrant further study.

Before discussing our calculations in detail, we feel that it is important to understand how they relate to previous work in this area. Nearly all of the previous discussions were expressed in terms of induced staggered fields. This emphasized the analogy between a "normal" system in the presence of a real staggered field and a system such as DAG which exhibits induced-staggered-field effects when subjected to only an ordinary (uniform) magnetic field. Although this analogy is a very useful one, we do not emphasize it in this paper. We are here concerned primarily with making quantitative estimates of the *effects* of the "induced staggered field," so as to determine the relative importance of various microscopic mechanisms. We therefore choose to emphasize quantities which are experimentally observable, such as the difference in the magnetizations of the two antiferromagnetic states. It is of course possible to re-express the results of our calculations in terms of an induced staggered field [as was done above in connection with Eq. (2)], but this in no way affects the calculations or any of the conclusions which we will draw from them. As a result, our paper contains calculations of the effects of the induced staggered field, but no calculations of the "size" of the induced staggered field itself, except for the rough estimate given in Eq. (2) above.

## II. MICROSCOPIC STRUCTURE AND INTERACTIONS IN DAG

### A. Structure

The structure of DAG is fairly complicated, with 24 spins per unit cell, as shown in Fig. 1.<sup>11-13</sup> However, the sites are all related by simple symmetry operations, and if, as throughout this paper, we restrict ourselves to the case of magnetic fields applied along a [111] crystal axis, we need consider only two inequivalent sites. These are shown schematically in Fig. 2. Other sites are related to these by simple 120° rotations about the [111] axis.

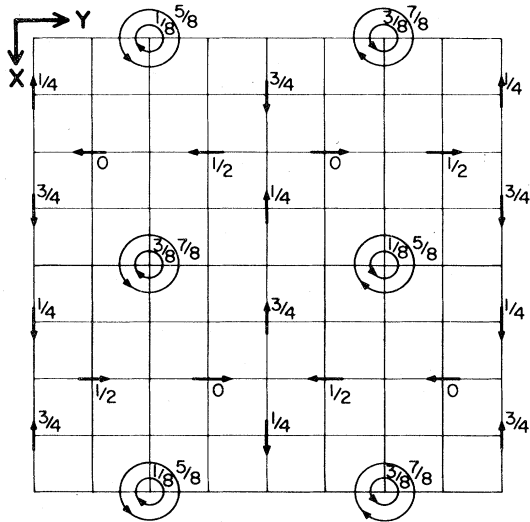


FIG. 1. Zero-field antiferromagnetic structure of DAG shown in a [001] projection of the unit cell (after Ref. 13). The numbers give the heights above the  $Z=0$  plane in terms of the unit-cell edge length. Spins pointing along  $Z$  are indicated by current loops with a right-hand sense. For fields directed along the [111] direction, this structure corresponds to the  $A^+$  antiferromagnetic state discussed in the text. The  $A^-$  state can be constructed by simply reversing the direction of every spin.

### B. Single-ion interactions

At the temperatures of interest in this paper, the ions may be represented<sup>4</sup> in terms of effective spins  $S = \frac{1}{2}$ , and the interaction of these with a magnetic field is described accurately by a magnetic  $g$  tensor whose principal axes for both of the sites shown in

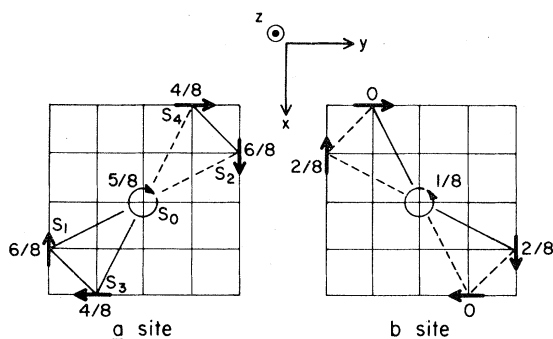


FIG. 2. Configuration of nearest-neighbor spins in DAG for sites on the two sublattices,  $a$  and  $b$ . The solid and dashed lines denote ferromagnetic and antiferromagnetic interactions, respectively. The notation is the same as that used in Fig. 1, with the exception that the spins around (and including) the  $a$  site are numbered in accord with the discussion in Sec. II C.

Fig. 2 are [110],  $[1\bar{1}0]$ , and [001] relative to the cubic crystal axes.<sup>14</sup> For one of the sites, which we shall denote as  $a$  (see Fig. 2), the principal  $g$  values corresponding to these axes will be  $g_x$ ,  $g_y$ , and  $g_z$ , while for the  $b$  sites they will be  $g_y$ ,  $g_x$ , and  $g_z$ .<sup>15</sup> For a field applied along the [111] direction, the effective  $g$  values for the two sites will thus be

$$g_a = \left( \frac{1}{3} g_z^2 + \frac{2}{3} g_x^2 \right)^{1/2} \quad (3a)$$

and

$$g_b = \left( \frac{1}{3} g_z^2 + \frac{2}{3} g_y^2 \right)^{1/2} \quad (3b)$$

For some rare-earth garnets, the values of  $g_x$  and  $g_y$  are quite large and quite different from one another, but in DAG both  $g_x$  and  $g_y$  are very small. There are no really accurate estimates for  $g_x$  and  $g_y$ , but experiments<sup>4</sup> have obtained an upper limit for the difference  $|g_x^2 - g_y^2| < 0.25$  which we shall need for our calculations. The third component,  $g_z$ , is large and well known, and its value is close to 18. For a further discussion of the  $g$  values and references to earlier work, see Ref. 4.

In addition to the first-order Zeeman effect characterized by the  $g$  tensor, there is also a second-order interaction with the magnetic field which results in the Van Vleck temperature-independent susceptibility. Microscopically, this susceptibility will also be anisotropic, with the same principal axes as the  $g$  tensor for each ion site. If we denote the principal values of the  $a$ -site ion in Fig. 2 as  $\alpha_x$ ,  $\alpha_y$ , and  $\alpha_z$ , the principal values of the  $b$ -site ions will be  $\alpha_y$ ,  $\alpha_x$ , and  $\alpha_z$ . The  $\alpha$ 's can in principle be calculated from the known wave functions,<sup>16</sup> but for our purposes it will suffice to estimate an upper limit for the difference  $|\alpha_x - \alpha_y|$ . This may be found simply by noting that the experimentally measured *bulk* Van Vleck susceptibility  $\chi_{VV}$  is related to our  $\alpha$ 's by

$$\chi_{VV} = \frac{1}{3} (\alpha_x + \alpha_y + \alpha_z) \quad (4)$$

and since all the  $\alpha$ 's are positive, we have

$$|\alpha_x - \alpha_y| \leq 3\chi_{VV} = 3.7 \times 10^{-3} \text{ emu/cm}^3 \quad (5)$$

using the results given in Ref. 4. This is a very small value, but, as we shall see, even if it were larger it could not explain the observed staggered-field effects.

There will, of course, also be higher-order interactions with the applied field, and in general we would expect these to be even smaller. Some of these could, in principle, contribute to the observed effects, but in DAG they will be so small that we shall neglect them. In very large fields, or in systems with low-lying electronic states, terms such as the fourth-order Zeeman effect could well be important.

### C. Interactions between ions

The description of the effective spin-spin interactions is more complex, and its discussion involves a number of unusual features. The most general form for the interaction of two spins  $\vec{S}_i = \frac{1}{2}$  and  $\vec{S}_j = \frac{1}{2}$  is

$$\mathcal{H}_{ij} = \vec{S}_i \cdot \vec{J}_{ij} \cdot \vec{S}_j, \quad (6)$$

where  $\vec{J}_{ij}$  is a tensor with nine independent terms. Previous work has established that in DAG one of these terms is dominant for each pair of spins, corresponding to the two spin components parallel to the *local*  $z$  axes of the  $g$  tensors at the two sites. One may thus describe the interactions as predominantly Ising-like, but with the implicit understanding that the  $z$  axes are not parallel in real space. In the absence of a magnetic field this presents no difficulty, since we are clearly free to choose an axis of quantization at each site. In the presence of an applied field, a more careful description is required, since the components of the field are fixed with respect to the *crystal* axes. In particular, one has to be careful about the relative signs of different interactions, in a way not recognized previously.<sup>17</sup>

Consider, for example, the interaction of the central  $a$ -site spin  $S_0$  in Fig. 2, with two of its nearest neighbors  $S_1$  and  $S_2$ . For the central spin, the local  $z$  axis corresponds to the crystal  $Z$  axis, but for  $S_1$  and  $S_2$  the local  $z$  axis is parallel to the crystal  $X$  axis. Under the influence of, say, magnetic-dipole interactions and the highly anisotropic  $g$  value, the spins will be aligned as shown. Relative to the *local* axes, one may describe spins  $S_0$  and  $S_1$  as ferromagnetically aligned; with an effective interaction  $-KS_0^z S_1^x$  and  $K > 0$ , whereas the pair  $(S_0, S_2)$  are antiferromagnetically aligned with an effective interaction  $+KS_0^z S_2^z$ .

Had we described all the interactions in terms of a common set of crystal axes, this difference would have followed directly from the symmetry. For the pair  $(S_0, S_1)$  the dominant interaction term would have appeared as  $K\alpha_{01}^z S_0^z S_1^x$ , which, under a rotation of  $180^\circ$  about the  $z$  axis, would transform to  $-K\alpha_{01}^z S_0^z S_1^z \equiv K\alpha_{02}^z S_0^z S_1^z$ . Thus  $K\alpha_{02}^z = -K\alpha_{01}^z$ , and if we identify the local  $z$  axes with  $Z$  and  $X$ , respectively, we get the change of sign noted previously.

Applying these considerations to other spin pairs, we get the arrangement of nearest-neighbor interactions shown in Fig. 2. We now note an interesting difference between the arrangement associated with  $a$  and  $b$  sites. In both cases, two of the nearest-neighbor interactions are ferromagnetic and two are antiferromagnetic, but the geometrical arrangement is different for the two types of sites. Specifically, we may note a triangle of spins  $(S_0, S_1, S_3)$  associated with an  $a$  site, in which all three nearest-neighbor interactions are ferromagnetic, while there is no similar triangle associated with the  $b$ -site spins.

The identification of ferromagnetic and antiferromagnetic bonds shown in Fig. 2 is of course not unique, since it depends on the signs of spin directions relative to a set of crystal axes, which is itself not unique. Thus, we have a choice of eight combinations of directions for the  $x$ ,  $y$ , and  $z$  axes, which we may characterize by the eight directions in space of the corresponding  $[111]$  axes. However, examination of the entire unit cell, shown in Fig. 1, reveals that four of these choices are really equivalent, while the other set of four corresponds to a reversal of all the spin directions shown in Figs. 1 and 2. The properties of the antiferromagnetic state  $A^-$  in a field along  $[111]$  thus correspond identically to those of the state  $A^+$  in a field along  $[\bar{1}\bar{1}\bar{1}]$ . We can therefore restrict ourselves to considering only the particular choice shown in Figs. 1 and 2 with  $\pm H$  along  $[111]$ .

A pattern of *staggered interactions* of this kind is not unique to the garnet lattice. Among the simplest examples of other lattices showing the same feature is two-dimensional Kagomé net with two ferromagnetic and two antiferromagnetic nearest-neighbor interactions. We have previously discussed the properties of such a system (see Giordano and Wolf in Ref. 17 and see Ref. 18) and have demonstrated that the principal staggered-field effects found experimentally in DAG are also properties of this simple model, even though the essential symmetries are somewhat different.<sup>18</sup>

In DAG, there are additional features of the interactions which must be taken into account for a complete description. First, we must consider the remaining eight terms in the interaction tensor  $\vec{J}_{ij}$  [Eq. (6)]. These non-Ising terms have been discussed in Ref. 4, and it has been shown that none of them is larger than about 3% of the dominant Ising-like terms. In view of the smallness of the staggered-field effects which we seek to explain, this is no guarantee that these terms will be negligible, but we will show in Sec. III C 1 that the effect of terms of such magnitude is, in fact, negligible in the present case. For other garnets, with less anisotropic interactions, staggered-field effects associated with some of the non-Ising terms could well be important. To include such effects, one would have to apply the same kind of symmetry considerations as discussed above to determine the relative signs of corresponding terms for various neighbors, and one would, of course, also have to estimate the sizes of the individual terms themselves. In practice, this can be quite difficult, and it is fortunate that DAG is described so well by an Ising model, albeit one with an unusual arrangement of ferromagnetic and antiferromagnetic interactions.

So far, we have discussed only the nearest-neighbor interactions, and these are indeed the dominant terms in DAG. However, there are also second- and third-nearest-neighbor interactions which are by no

TABLE I. Interaction constants for first-, second-, and third-nearest neighbors,  $K_1$ ,  $K_2$ , and  $K_3$ , and the  $T = H = 0$  excitation energy,  $\Delta$  taken from Refs. 4 and 19. Note that the  $K_i$  are normalized such that  $2K_i$  is the energy required to reverse an  $i$ th nearest-neighbor spin.

$K_1/k_B$	$K_2/k_B$	$K_3/k_B$	$\Delta/k_B$
0.770 K	0.159 K	-0.402 K	7.54 K

means negligible, and in any quantitative calculations we shall also have to include these. As in the case of the nearest neighbors, the major part of the interactions is specified by one parameter per pair, and values for these have been estimated from experimental data by Schneider *et al.*<sup>19</sup> The results are summarized in Table I, where  $K_1$  denotes the interaction parameter for first-nearest neighbors, etc. For fourth and more distant neighbors, the interactions may be calculated to sufficient accuracy<sup>20</sup> simply from the magnetic-dipole coupling, taking into account the highly anisotropic  $g$  tensor.

In summary, then, we may describe DAG in a field  $H$  along [111] by an interaction Hamiltonian which has the form

$$\mathcal{H} = \mathcal{H}_I + \sum_{k=1}^4 V_k, \quad (7a)$$

where

$$\mathcal{H}_I = -\left(\frac{1}{3}\right)^{1/2} \mu_B H g_z \sum_i S_i^z + \sum_{\langle ij \rangle} K_{ij} S_i^z S_j^z, \quad (7b)$$

$$V_1 = -\left(\frac{2}{3}\right)^{1/2} \mu_B H g_x \sum_{i-a} S_i^x - \left(\frac{2}{3}\right)^{1/2} \mu_B H g_y \sum_{i-b} S_i^y, \quad (7c)$$

$$V_2 = \sum_{\langle ij \rangle} \sum_{\alpha=x,y} J_{ij}^{\alpha z} S_i^\alpha S_j^z, \quad (7d)$$

$$V_3 = \sum_{\langle ij \rangle} \sum_{\alpha, \beta=x,y} J_{ij}^{\alpha \beta} S_i^\alpha S_j^\beta, \quad (7e)$$

$$V_4 = -\sum_{i-a} \frac{1}{2} \left( \frac{1}{3} \alpha_z + \frac{2}{3} \alpha_x \right) H^2 1_i - \sum_{i-b} \frac{1}{2} \left( \frac{1}{3} \alpha_z + \frac{2}{3} \alpha_y \right) H^2 1_i, \quad (7f)$$

where  $\langle ij \rangle$  denotes a sum over all pairs of spins, the  $1_i$  denote unit operators at the  $i$ th site, and we assume implicitly that only the lowest Kramers doublet of each ion is populated under the conditions to be considered ( $T \ll 100$  K). At higher temperatures, additional effects due to excited crystal-field states will, of course, become important.

The leading term  $\mathcal{H}_I$  in Eq. (7a) has the form of a single-axis Ising model used previously,<sup>4</sup> but with the

understanding that the signs of the individual pair interactions  $K_{ij}$  are to be determined according to the symmetry considerations discussed above. The terms in the  $V_k$  represent various deviations from a simple Ising model. We shall find that *none* of these is in fact important for the effects which have been observed in DAG so far, but they may become significant at higher and lower temperatures, and also in other systems.

### III. LOW-TEMPERATURE EFFECTS

One of the simplest and most reliable methods of treating a Hamiltonian such as Eq. (7a) is to consider the energy of the ground state and the low-lying excitations. If we treat the  $V_k$  as perturbations, it is easy to find the unperturbed states, since the energy levels of the Ising Hamiltonian [Eq. (7b)] can be written by considering various simple spin configurations.

The antiferromagnetic ground-state configuration of DAG is well known theoretically<sup>11</sup> and experimentally<sup>12,13</sup> and it is simply an extension of the patterns shown in Fig. 2, as indicated in Fig. 1. Its energy  $E_0$  is independent of field, and we shall measure all energies relative to  $E_0$ . The excited states correspond to one, two, three, etc., spins reversed relative to their orientation in the ground state, and we shall calculate the energies of these states as we need them.

#### A. $g$ -value mechanism

This is the mechanism which was first suggested by Blume *et al.*,<sup>6</sup> and it corresponds to the term  $V_1$  in Eq. (7c). The microscopic origin of this mechanism can be seen most clearly by considering Eqs. (3a) and (3b). Since all of the spins on the  $a$  sublattice couple to the field with the  $g$  value  $g_a$ , and all of the spins on the  $b$  sublattice couple with  $g_b$ , and since  $g_a \neq g_b$ , this will lead to an effect equivalent to that of an induced staggered field. Foglio and Blume<sup>10</sup> have recently considered this mechanism using a mean-field approximation, but their calculation was essentially a numerical one, and it is hard to compare their results with those of the other mechanisms considered here.

It is easy to find the perturbation of the ground state due to  $V_1$ . Since  $V_1$  is composed solely of single factors of  $S_i^x$  or  $S_i^y$ , it will have no diagonal matrix elements within the eigenstates of  $\mathcal{H}_I$  and thus to first order  $V_1$  will have no effect on the ground-state energy. It will, however, contribute in second order since it will mix the ground state with the excited states in which one spin is flipped from the ground state. A straightforward calculation (given in Appendix A) shows that to second order in the perturbation and to lowest order in the field, the ground-state

energy is

$$E_g = E_0 - \frac{1}{12} N (\mu_B^2 H^2 / \Delta) (g_x^2 + g_y^2) - (N \mu_B^3 / 12 \sqrt{3} \Delta^2) g_z (g_x^2 - g_y^2) H^3, \quad (8)$$

where  $N$  is the total number of spins and  $\Delta$  is the energy required to flip one spin at  $T=0$  and  $H=0$ . If we had considered instead the effect of  $V_1$  on the time-reversed antiferromagnetic ground state  $A^-$ , we would have obtained the same expression as Eq. (8), but with  $H$  replaced by  $-H$ . We see, therefore, that the third term in Eq. (8) has the form corresponding to Eq. (1), and it will contribute to the induced-staggered-field effects predicted on the basis of symmetry. As predicted,<sup>7</sup> there is no linear term in  $H$ .

Before we can compare the effect of this mechanism with experiment, it is necessary to extend the calculation to finite temperatures. This involves considering excited states with one and two spins flipped and finding the corresponding perturbed energies. Using these to calculate the partition function  $Z$ , one then finds the free energy  $F$  from which other thermodynamic functions can be determined. Details of the calculation are given in Appendix A. The results show that the leading terms in the expansion of  $F$  has the form

$$F = E_g - \frac{1}{2} N k_B T [\exp(-\Delta_x / k_B T) + \exp(-\Delta_y / k_B T)], \quad (9a)$$

where

$$\Delta_x = \Delta - g_z \mu_B H / \sqrt{3} + (\mu_B^2 H^2 g_x^2 / 3 \Delta) \times (1 + g_z \mu_B H / \sqrt{3} \Delta), \quad (9b)$$

$$\Delta_y = \Delta + g_z \mu_B H / \sqrt{3} + (\mu_B^2 H^2 g_y^2 / 3 \Delta) \times (1 - g_z \mu_B H / \sqrt{3} \Delta).$$

$E_g$  is the ground-state energy given by Eq. (8), and  $k_B$  is Boltzmann's constant. Previous experiments have shown<sup>4</sup> that  $\Delta = 7.5 k_B$ , and for reasonably low temperatures and fields the effect of the additional terms due to the excited states will therefore be quite small.

From Eq. (9a) we can calculate the magnetization using  $M = -\partial F / \partial H$ , and we can thus find the difference in magnetization  $\Delta M$  of the  $A^+$  and  $A^-$  states in a field.  $\Delta M$  can then be compared with the experimental results of Dillon *et al.*<sup>9</sup> To lowest order in  $H$  we find

$$\Delta M / M_0 = (\mu_B^3 / \Delta^2) (g_x^2 - g_y^2) H^2 \times [1 - 2e^{-\Delta / k_B T} (\Delta / k_B T + 1)], \quad (10)$$

where  $M_0 = N \mu_B g_z / 2 \sqrt{3}$  is the saturation magnetization. To compare Eq. (10) with the experiments, we substitute for  $\mu_B$  and  $\Delta$ , put  $(g_x^2 - g_y^2) = 0.25$ , the

TABLE II. Comparison of the experimental results for the difference  $\Delta M$  in the magnetizations of the two antiferromagnetic states measured at  $H = 2.5$  kOe, with the values predicted on the basis of the  $g$ -value effect [Eq. (10)] and assuming  $(g_x^2 - g_y^2) = 0.25$ .

$T$ (K)	$\frac{\Delta M(\text{obs})}{M_0}$ (Ref. 9)	$\frac{\Delta M(\text{calc})}{M_0}$ [Eq. (10)]
1.32	$7(\pm 4) \times 10^{-4}$	$1.18 \times 10^{-4}$
1.50	$1.5(\pm 0.4) \times 10^{-3}$	$1.14 \times 10^{-4}$
1.80	$6.0(\pm 0.4) \times 10^{-3}$	$1.04 \times 10^{-4}$

largest value allowed, and evaluate the expression for  $H = 2.5$  kOe and  $T = 1.32, 1.50$ , and  $1.80$  K. The results are shown in Table II.

It is clear that the  $g$ -value mechanism is quite inadequate to account for the observations. Not only is the absolute magnitude much too small, but also the temperature dependence is much too weak. These failures cannot be ascribed to approximations in the calculation, which should be quite accurate, or to errors in the parameters, which are all well known, and we must conclude that the  $g$ -value mechanism itself is not the correct mechanism to account for at least these experiments. A similar conclusion was also reached by Foglio and Blume,<sup>10</sup> who considered the induced antiferromagnetic order at higher temperatures.

Nevertheless, it would be wrong to conclude that the  $g$ -value mechanism is always inadequate to account for observable induced-staggered-field effects in DAG. In particular, we note that the effect tends to a constant value as  $T \rightarrow 0$  K, which is not the case for the other major mechanism which we shall consider next. Thus, at very low temperatures we would expect the  $g$ -value mechanism to become dominant, and we shall discuss some consequences of this in Sec. III D.

It is also worth pointing out that the  $g$ -factor difference  $(g_x^2 - g_y^2)$  can be two or three orders of magnitude larger in other rare-earth garnets [e.g., dysprosium gallium garnet (see Wolf *et al.* in Ref. 15)] so that the  $g$ -value mechanism may produce some large effects in other systems.

### B. Staggered-interaction mechanism

Here we consider some of the consequences arising from the pattern of staggered interactions which we noted in Sec. II. These consequences are not immediately obvious since it turns out that there are no effects if we use a mean-field type of approximation.

Also, as we shall see, in a low-temperature series expansion there are no effects until we consider terms involving the simultaneous excitation of *three* neighboring spins. This is not entirely unexpected, since we know from symmetry that the lowest-order term in the free energy related to the staggered-field effects is proportional to  $H^3$ , so that it is not unreasonable to look for excitations involving three spins. This may explain why the effect has not been noted before.

Let us first examine the construction of a low-temperature-low-field series expansion for the magnetization from a qualitative point of view. Starting from either the  $A^+$  or the  $A^-$  ground state and considering the energy of excitations in which one spin is flipped, it is easy to show that these will occur with equal probability from either ground state. Excitations involving two spins will also occur with equal probability in each of the two antiferromagnetic states. However, if we consider excitations of three or more spins, then the two antiferromagnetic states are no longer equivalent. In particular, we see that for one state  $A^+$  it is possible to have an excitation in which a cluster of three spins which are all nearest neighbors of each other ( $S_0$ ,  $S_1$ , and  $S_3$  in Fig. 2) are flipped to become parallel to the field. On the other hand, such an excitation is not possible from the other ground state  $A^-$ , since in this state all of these clusters are already parallel to the field. The two antiferromagnetic states will therefore have different magnetizations. They will also have different free energies and hence only one of them will be stable. However, the other state will probably be metastable, since in order to pass from one state to the other it is necessary to flip nearly every spin. If the field is reversed, the other antiferromagnetic state will become stable, and hence we have the basis for the observed hysteresis.

These ideas can be made quantitative by enumerating all of the relevant excitations and constructing series expansions for the magnetizations of the two sublattices  $M_{\pm}$ . The calculation is complicated somewhat by the presence of dipolar interactions and the associated demagnetizing effects. To deal with these, we allow the fields acting on the two sublattices to be unequal and include the effects of third- and more-distant-neighbor interactions by the introduction of two mean fields  $H_{\pm}$ , which can be calculated from the known interactions. Improvements on this approach are clearly possible, but, as we will see, the approximation suffices to give good quantitative agreement with the available observations.

Details of the calculation are given in Appendix B, and the results are shown as the broken lines in Fig. 3. It can be seen that the agreement with the experimental magnetization measurements of Dillon *et al.*<sup>9</sup> is good, both with respect to the magnitude and temperature dependence of the effect. The agreement is

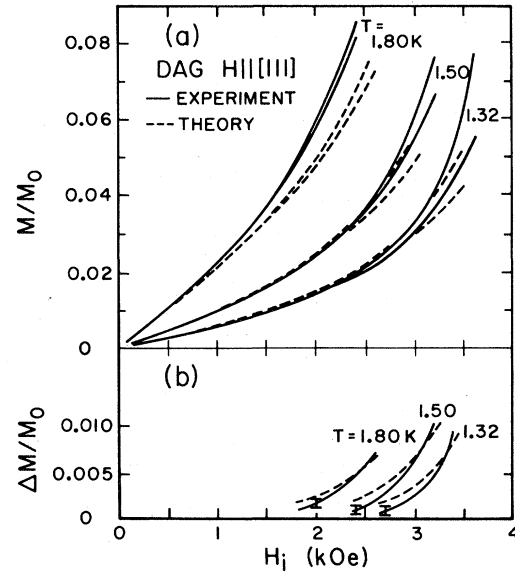


FIG. 3. Comparison of the experimental results of Dillon *et al.* (Ref. 9) for (a) the magnetizations of the two antiferromagnetic states  $M$ , and (b) the difference in the magnetizations  $\Delta M$ , with the theoretical predictions based on the staggered-interaction mechanism.

especially satisfactory considering that the theory contains no adjustable parameters. The small residual discrepancies can almost certainly be ascribed to the truncation of the series and the mean-field approximation for the more distant neighbors. We conclude, therefore, that the staggered-interaction mechanism is principally responsible for the low-field effects observed by Dillon *et al.*<sup>5,9</sup>

### C. Other mechanisms

#### 1. Non-Ising interactions

The terms  $V_2$  and  $V_3$  in Eq. (7) represent interactions which will couple different states of the unperturbed-Ising-model Hamiltonian, and which in some sense may therefore act similarly to the off-diagonal Zeeman terms in  $V_1$ . To obtain an estimate of their effect at low temperatures, we shall first consider the change in ground-state energy, as in Sec. III A.

Since we know from symmetry considerations that the leading term which we seek will be proportional to  $H^3$ , we can start by examining qualitatively what kind of perturbation term will in fact lead to such a field dependence. In second order, the contribution to the ground-state perturbation by one of the terms in  $V_2$  or  $V_3$  will be of order  $(J^{\alpha\beta})^2/(-E_i)$ , where  $E_i$  is the energy of the appropriate excited state. It is evident that the only field dependence will come from the variation of the  $E_i$ , which for Ising-model

states will be of the form  $\Delta_i - n_i \mu H$ , where  $\Delta_i$  is the zero-field energy gap,  $n_i$  is an integer corresponding to the magnetic moment of the excited state, and  $\mu = g_z \mu_B / 2\sqrt{3}$ . To obtain a contribution in  $H^3$  one must expand the denominator, and the leading term of interest will therefore have the form  $(J^{\alpha\beta})^2 (\mu H)^3 / \Delta_i^4$ . This is clearly very small. The  $\Delta_i$  are typically of the order of  $\Delta$ , the energy to reverse one spin which as discussed above is  $7.5 k_B$ . The individual  $J^{\alpha\beta}$  on the other hand, are smaller than 3% of the Ising  $K$ 's and hence less than  $0.03 k_B$ . The ratio of one of these terms to the corresponding  $g$ -tensor contribution [Eq. (8)] will therefore be of order

$$\frac{(J^{\alpha\beta})^2 g_z^2}{\Delta^2 (g_x^2 - g_y^2)} \sim \frac{(0.03)^2 (18^2)}{(7.5)^2 (0.25)} \sim 0.02, \quad (11)$$

where we have ignored all matrix element factors of order unity. Using our best estimate for the various parameters, we see that the contribution from the non-Ising terms will indeed be very much smaller than that of the  $g$ -tensor mechanism, which itself was much too small to account for the observations in DAG.

Higher-order perturbation terms will generally be even smaller since they will contain extra factors  $J^{\alpha\beta}$ , and even though some of the energy denominators could be less than  $\Delta$ , it seems unlikely that the higher-order terms would dominate the second-order contribution which we have considered. It would seem therefore that it is not worth calculating the non-Ising contributions in any more detail at this time and that we can safely ignore them in accounting for the observations in DAG.

However, as in the case of the  $g$ -tensor mechanism, it is useful to note that the effect of the non-Ising terms might well be important in other systems for which the  $J^{\alpha\beta}$  parameters could be much larger. Also, of course in relation to the  $g$ -tensor mechanism one might consider the possibility that  $(g_x^2 - g_y^2)$  might be even smaller than in DAG, so that the relative importance of the non-Ising terms might be greater, but the absolute magnitude of observable effects would still be very small.

## 2. Van Vleck susceptibility

This was one of the two mechanisms mentioned by Blume *et al.*,<sup>6</sup> and it is one whose effect can be derived readily. As we have seen in Sec. II, the Van Vleck susceptibility will be different for ions at the  $a$  and  $b$  sites, and in the presence of a field along [111], the induced moments will be different. For both sites, the component along [001] will be  $\alpha_x H / \sqrt{3}$ , but along [110] the moment for the  $a$  site shown in Fig. 2 will be  $(\frac{2}{3})^{1/2} \alpha_x H$ , while for the  $b$  site it will be  $(\frac{2}{3})^{1/2} \alpha_y H$ . The field will thus produce

an induced staggered magnetization with amplitude  $(\frac{2}{3})^{1/2} (\alpha_x - \alpha_y) H$  along [110]. For other  $a$  and  $b$  sites similar moments will be induced along the [101] and [011] directions.

We note that all these directions are perpendicular to the local  $z$  axes, and these induced moments will therefore not contribute to the order parameter characterizing the antiferromagnetism in DAG. This is really not surprising, since this induced moment is linearly proportional to  $H$ , whereas we know from the symmetry arguments<sup>7</sup> that the DAG order parameter  $M_s$  ( $\eta$  in the notation of Ref. 7), is only coupled to  $H^3$  and higher powers of  $H$ .

There are, of course, many other order parameters in a system as complex as DAG. These have recently been enumerated in detail Mukamel and Blume,<sup>21</sup> who have shown that in DAG there are altogether 18 order parameters which will couple to an applied field. We can identify the induced staggered magnetization resulting from the Van Vleck susceptibility with a combination of two of these other order parameters<sup>22</sup>  $M_{3x}$  and  $M_{3y}$ , both of which are coupled linearly to  $H$ .

To obtain a contribution to the antiferromagnetic order parameter  $M_s$  from the Zeeman effect, we would have to consider interaction terms involving  $H^4$ , and these will generally be extremely small. In DAG their effect would certainly be very hard to observe, but in other systems with low-lying crystal-field levels they could become significant. Also, we should note that the higher-order Zeeman terms will be independent of temperature, so that their effect could become dominant at high temperatures where, as we shall see, all other mechanisms vanish as  $T \rightarrow \infty$ . However, for all the experiments reported so far, we may safely neglect the Van Vleck susceptibility and higher-order Zeeman effects.

## D. Competition between different mechanisms

The mechanisms which we have considered in Secs. III A–III C differ not only in magnitude but also in their dependence on temperature. This gives rise to the possibility of some interesting competition effects which we shall consider here. None of these effects has been observed as yet, and, even if they occur, it may be quite difficult to observe them in DAG. However, it seems quite likely that they will be observable in other systems, and it is therefore useful to consider some of the qualitative effects which may be expected.

Table III summarizes the temperature dependence of the four mechanisms which may contribute to staggered-field effects. (For completeness, we also give the high-temperature behavior as derived in Sec. IV.) Associated with each mechanism is a *sign* which



TABLE III. Temperature dependence of the different induced-staggered-field mechanisms.

Mechanism	$T=0$	Low $T$	High $T$
$g$ -value mechanism	finite	slow	$T^{-3}$
Staggered interactions	0	rapid	$T^{-6}$
Non-Ising interactions	finite	slow	$T^{-6}$
Higher-order Zeeman effect	finite	constant	constant

corresponds to either the  $A^+$  or  $A^-$  state being stabilized. In the absence of more detailed information about the parameters in the microscopic Hamiltonian [Eq. (7)], it is not possible to determine these signs in general, but it is certainly quite likely that some of the mechanisms will have signs different from the rest. Since all the mechanisms have different temperature dependences, the total effect, i.e., the sign of the induced staggered field, can change one or more times as the temperature is increased. With four active mechanisms, quite complicated variations with temperature are clearly possible.

In DAG, two of the mechanisms are probably much weaker than the other two, as we have seen, and at low temperatures the principal competition will be between the  $g$  value and staggered interaction mechanisms. We can therefore consider two main cases.

*Case 1.* If  $g_x > g_y$ , the two mechanisms will favor the same antiferromagnetic state ( $A^+$  for  $H > 0$ ; see

Fig. 1) and no qualitatively new effects would be expected.

*Case 2.* On the other hand, if it should happen that  $g_x < g_y$ , the two mechanisms will favor different antiferromagnetic states, and competition may be expected. In this case, the ordered state at sufficiently low temperatures will be determined by the  $g$ -value mechanism, since this remains finite as  $T \rightarrow 0$  while the staggered interaction mechanism goes to zero as  $T \rightarrow 0$  K. However, as the temperature is raised, the effect of the staggered interaction mechanism will increase rapidly [Eq. (B3)] while that of the  $g$ -value mechanism varies only slowly [Eq. (10)] and one may expect to find a point where the two effects just cancel. If the cancellation occurs at a temperature *below* the Néel point (which as we will see shortly will be the case in DAG if  $g_x < g_y$ ) it will lead to a first-order phase transition, corresponding to a discontinuous change from the state  $A^+$  to the state  $A^-$  as the temperature is increased.

These ideas can be made quantitative in the case of DAG. Using the expressions previously obtained for the free-energy contributions from the two mechanisms [Eqs. (9) and (B2)], we can find the locus of points at which the two just cancel. Anticipating the fact that the temperatures will turn out to be quite low ( $\sim 1$  K) where both sublattices are close to saturation, we can simplify the previous expressions by putting  $M_+/M_0 = \frac{1}{2}$  and  $M_-/M_0 = -\frac{1}{2}$ , and setting  $C = \exp(-2\mu H_0/k_B T)$ ,  $D = \exp[(\lambda_1 - \lambda_2)/k_B T]$ , with  $A$  and  $B$  as defined in Appendix B. We obtain

$$F = -k_B T \ln Z = E_{gs} - Nk_B T \left[ \frac{1}{2} A^2 B^4 D (C + C^{-1}) + \frac{1}{2} A^3 B^8 D^2 (C^2 + C^{-2}) + A^4 B^7 D^2 (C^2 + C^{-2}) - \frac{7}{4} A^4 B^8 D^2 (C^2 + C^{-2}) + \frac{1}{6} A^3 B^{12} D^3 C^{-3} + \frac{1}{2} A^4 B^{12} D^3 C^3 + \frac{1}{2} A^3 B^{12} D^3 C + A^4 B^{12} D^3 C + \frac{5}{2} A^4 B^{12} D^3 C^{-1} \right], \quad (12)$$

where we have dropped those terms which are independent of  $H$  as they will not contribute to the effect of interest and we have also omitted the small temperature-dependent terms in Eq. (9).

The difference in the free energies of the two antiferromagnetic states is just  $\Delta F = F(H) - F(-H)$ , which from Eq. (12) is given by

$$\Delta F = -N \mu_B^3 g_z (g_x^2 - g_y^2) H^3 / 6\sqrt{3} \Delta^2 - \frac{1}{6} N A^3 B^{12} D^3 k_B T [(C^{-3} - C^3) + 3(C - C^{-1})], \quad (13)$$

where we have now also dropped the terms in  $A^4$ , since these will be small at the low temperatures of interest (at  $T = 1.2$  K,  $A \sim 0.1$ ). Setting  $\Delta F = 0$  finally gives the locus of the phase boundary between the  $A^+$  and  $A^-$  states.

For low fields,  $C$  can be expanded in powers of  $H$ ,

and we find that the leading terms in  $\Delta F$  are proportional to  $H^3$ , as we would expect:

$$\Delta F = -\frac{N \mu_B^3 g_z}{6\sqrt{3} \Delta^2} (g_x^2 - g_y^2) H^3 - \frac{N A^3 B^{12} D^3}{(k_B T)^2} \frac{4}{9\sqrt{3}} \mu_B^3 g_z^3 H^3 = -\frac{N \mu_B^3 g_z H^3}{6\sqrt{3}} \left[ \frac{g_x^2 - g_y^2}{\Delta^2} + \frac{8g_z^2}{3(k_B T)^2} \right] \times \exp \left[ \frac{-12K_1 - 48K_2 + 3\lambda_1 - 3\lambda_2}{k_B T} \right] \quad (14)$$

The temperature  $T_1$  at which  $\Delta F = 0$  in the limit  $H \rightarrow 0$  is found by setting the coefficient of  $H^3$  to zero, and substituting for the various parameters we obtain  $T_1 \leq 1.15$  K, where the upper limit corresponds to the maximum value of  $|g_x^2 - g_y^2| = 0.25$ .

To find the field dependence of the phase bound-

dary, we set  $\Delta F = 0$  in Eq. (13) and solve for  $T$  as a function of  $H$ . The results, again assuming  $|g_x^2 - g_y^2| = 0.25$  are shown in Fig. 4. The uncertainty due to the finite number of terms in the series was estimated by recalculating the location of the phase boundary including the terms proportional to  $A^4$  which were previously dropped, and comparing the results of the two approximations. The difference was found to be about the thickness of the line in Fig. 4, and it seems safe to conclude that other higher-order terms would not change the location of the phase boundary significantly.

Figure 4 also shows the first-order phase boundaries studied in previous work,<sup>1</sup> where we have extended the conventional phase diagram to include both positive and negative fields to emphasize the unusual topology. We see that there are, in addition to the previously recognized critical points ( $T_N$ ,  $T_c$ , and  $T_c'$ ), also two triple points (TP and TP') where three phases coexist [ $(P^+, A^+, A^-)$  and  $(P^-, A^+, A^-)$ ] and a point ( $T_1$ ) where two lines of first-order transitions cross.

In Fig. 4 we also indicate schematically the second

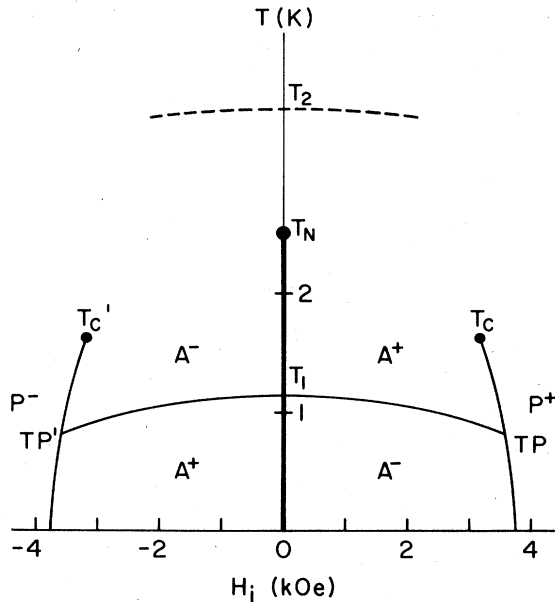


FIG. 4. Phase diagram for DAG for the case  $g_x < g_y$  described in the text. The  $A^+$  and  $A^-$  phases are at low temperatures and nonzero fields separated by a first-order phase boundary across which the order parameter changes discontinuously. The other heavy lines separating the  $P^\pm$  and  $A^\pm$  phases are the first-order transitions studied extensively in earlier work (Ref. 1-3). The dashed line passing through  $T_2$  indicates schematically the second change of sign of the order parameter which would be expected at higher temperatures. Note that the phase diagram for temperatures below  $T_N$  is drawn to scale for DAG assuming  $g_x^2 - g_y^2 = -0.25$ .

change in sign of  $M_s$  which is expected at higher temperatures, where the  $g$ -value mechanism will again determine the ordering. It is more difficult to give a quantitative estimate for the value of  $T_2$ , the temperature at which the two competing mechanisms will become equal again, but it is clear that the  $g$ -value mechanism will ultimately dominate, since it depends on temperature only as  $T^{-3}$ , whereas the staggered interaction mechanism varies as  $T^{-6}$  (see Sec. IV). Depending on the relative strengths of the two mechanisms,  $T_2$  could fall either above or below  $T_N$ . For  $T_2 < T_N$ , the locus of points corresponding to the change of sign of  $M_s$  will again be a first-order transition, while for  $T_2 > T_N$  it simply represents points at which the induced antiferromagnetic order is zero. In general,  $T_2$  (as well as  $T_1$ ) could also lie near  $T_N$ , and this might result in some unusual features in the thermodynamic behavior and the corresponding phase diagram.

It would clearly be of interest to determine which of these possible cases applies to DAG. Unfortunately, it is very difficult to predict the sign of  $(g_x^2 - g_y^2)$ , so that there is really no way of deciding *a priori* whether the two mechanisms will compete at all. An experimental study of the phase diagram itself is probably also quite difficult since there are indications<sup>23</sup> that the relaxation between the antiferromagnetic phases is very slow at low temperatures, with time constants of the order of hours for  $T < 1.3$  K. We would expect the relaxation time to become even longer at lower temperatures and this would make it extremely difficult to locate the  $(A^+, A^-)$  phase boundary directly. It may, however, be possible to determine the presence or absence of the  $(A^+, A^-)$  phase boundary indirectly by making use of the adjoining first order  $(A, P)$  phase boundaries, across which equilibrium is established much more rapidly.<sup>5,9,23</sup> Further work is clearly needed on these and other possible effects resulting from competing induced-staggered-field mechanisms.

#### IV. HIGH-TEMPERATURE EFFECTS

Before we can discuss "high"-temperature effects meaningfully, we must note two scales against which we might measure the size of  $k_B T$ . One is set by the strength of the spin-spin interactions, which are of the order  $K_n$ , while the other is set by the Zeeman interactions, which are of order  $\mu H$ . Since the field is readily varied, one can therefore consider two different limiting "high-temperature" regimes defined by

$$k_B T \gg \mu H, K_n \quad (15a)$$

and

$$k_B T, \mu H \gg K_n \quad (15b)$$

The first of these, clearly lends itself to the usual kind of high-temperature series expansion of the partition function in terms of  $\beta = 1/k_B T$ , with coefficients which are powers of  $\mu H$  and the  $K_n$ . In the second, one treats the field exactly in terms of a single-spin picture, with the interactions  $K_n$  added as a perturbation.<sup>24</sup>

Since there are no experimental high-temperature results at this time, we shall not carry out any detailed calculations, but it is useful to consider qualitatively the kinds of terms which will be important.

For the staggered-interaction mechanism, which depends on multiple-spin correlations, we know that we need at least three factors involving the spin-spin interactions, while the group theory indicates that the lowest-order term must be cubic in  $H$ . We may expect, therefore, that the leading term in any series expansion for, say, the order parameter will be of the form

$$M_s/M_0 \sim (K_n)^3 (\mu H)^3 / (k_B T)^6 . \quad (16)$$

For the  $g$ -value mechanism, on the other hand, the leading term would be expected to be independent of the  $K_n$  and simply proportional to  $H^3$ ,

$$M_s/M_0 \sim (\mu H)^3 / (k_B T)^3 , \quad (17)$$

with a coefficient which depends on the difference between  $g_x$  and  $g_y$ .

Comparing Eqs. (17) and (18) we see at once that the  $g$ -value mechanism will always dominate over the staggered interaction mechanism at high temperatures, just as it did at very low temperatures.

To estimate the magnitude of the field-induced order parameter at high temperatures, it is simplest to consider the regime represented by Eq. (15b), which applies to the case of relatively high fields. For this, one treats the field exactly, neglecting the spin-spin interactions as a first approximation, reducing the problem to a trivial single-spin calculation. Since this corresponds in effect to considering only the  $g$ -value mechanism, the result will also apply at lower fields for sufficiently high temperatures.

For an anisotropic spin  $S = \frac{1}{2}$  in a field  $H$ , the magnetization along the local  $z$  axis of the  $g$  tensor is given by

$$M_z = \frac{1}{2} g_e \mu_B \left[ \tanh \left( \frac{g_e \mu_B H}{2 k_B T} \right) \right] \frac{g_z^2 H_z}{g_e^2 H} , \quad (18)$$

where  $g_e$  is given through the relation

$$g_e H = (g_x^2 H_x^2 + g_y^2 H_y^2 + g_z^2 H_z^2)^{1/2} . \quad (19)$$

For the case of  $H \parallel [111]$  and  $g_x \neq g_y$ , the effective  $g$  values for the  $a$  and  $b$  sites are different, as given by Eq. (3), and hence there will be a difference in the two sublattice magnetizations. The order parameter

$M_s$  is equal to this difference

$$M_s = \sum_{i=a} M_{zi} - \sum_{i=b} M_{zi} \quad (20)$$

and hence,

$$M_s = \frac{1}{2} N \left( \frac{1}{2} \mu_B \right) \left\{ g_a \left[ \tanh \left( \frac{g_a \mu_B H}{2 k_B T} \right) \right] \frac{g_z^2 H_z}{g_a^2 H} - g_b \left[ \tanh \left( \frac{g_b \mu_B H}{2 k_B T} \right) \right] \frac{g_z^2 H_z}{g_b^2 H} \right\} . \quad (21)$$

Substituting  $H_z = H/\sqrt{3}$ , this reduces to

$$M_s = \frac{N \mu_B g_z^2}{4\sqrt{3}} \left[ \frac{1}{g_a} \tanh \left( \frac{g_a \mu_B H}{2 k_B T} \right) - \frac{1}{g_b} \tanh \left( \frac{g_b \mu_B H}{2 k_B T} \right) \right] . \quad (22)$$

This expression can be evaluated for all  $H$  and  $T$  using the known  $g$  values. One can also expand the tanh's to find the leading terms, and after a little rearranging this gives

$$M_s = -N \mu_B^4 g_z^2 (g_x^2 - g_y^2) H^3 / 144 \sqrt{3} (k_B T)^3 . \quad (23)$$

As expected from our earlier discussion this is proportional to  $H^3$  and  $1/T^3$  and it is also proportional to the difference  $(g_x^2 - g_y^2)$ . The negative sign in Eq. (23) shows that a field in the  $[111]$  direction will induce the antiferromagnetic state  $A^+$  if  $(g_x^2 - g_y^2) > 0$ , as was the case for the  $g$ -value mechanism at low temperatures [see Eq. (8)]. Substituting typical values  $H = 5$  kOe and  $T = 4$  K, and taking  $(g_x^2 - g_y^2) = 0.25$ , this gives

$$M_s/M_{s0} = -2 \times 10^{-5} , \quad (24)$$

where  $M_{s0}$  is the saturation value for the staggered magnetization

$$M_{s0} = \frac{1}{2} N \mu_B g_z . \quad (25)$$

For larger values of  $H$  one must use the complete expression given in Eq. (22) which leads to a limiting value

$$\lim_{H \rightarrow \infty} \left( \frac{M_s}{M_{s0}} \right) = \frac{1}{2} \left[ \left( 1 + \frac{2g_x^2}{g_z^2} \right)^{-1/2} - \left( 1 + \frac{2g_y^2}{g_z^2} \right)^{-1/2} \right] . \quad (26)$$

and taking  $g_x = 0.5$ ,  $g_y = 0$ , and  $g_z = 18$ , this gives

$$(M_s/M_{s0})_{\max} = -3.9 \times 10^{-4} , \quad (27)$$

still a very small value.

These results show that high-temperature effects will be very hard to observe in DAG, and it is clearly

not worthwhile, at this stage, to consider the small change which would result from the inclusion of the neglected interaction terms. In other systems, with less extreme  $g$ -value anisotropy, the field-induced staggered magnetization could be very much larger, and we shall discuss some of these in Sec. VI.

We have so far discussed the high-temperature effects of only the  $g$  value and staggered-interaction mechanisms, since these appear to be dominant in DAG under normal circumstances. It may be worth pointing out, however, that effects such as the non-Ising interactions and higher-order Zeeman terms mentioned in Sec. III C could well become important under extreme conditions, since their field and temperature dependences will generally be different from those of the other effects. In practice, it seems quite unlikely that one could observe any induced order arising from such effects directly in DAG, but it might turn out that the sign of the order parameter corresponding to such an effect at very high temperatures might, in a given experiment, be important in determining the sign of the order at lower temperatures. In other systems both the higher-order Zeeman terms and the non-Ising interactions could well contribute directly to observable induced-staggered-field effects, but we shall not pursue this possibility here.

## V. INTERMEDIATE TEMPERATURES

At temperatures which are neither very high nor low compared to  $T_N$  or  $\mu H$ , one has the usual difficulties with statistical approximations. It is tedious to extend the exact series expansions, while simple approximations such as mean-field theory can miss significant features of a problem. In particular, one must be careful not to ignore the effect of multiple-spin correlations, which result from the staggered-interaction mechanism in the present case. To obtain quantitative results at intermediate temperatures, we have therefore used a cluster approximation, chosen to ensure the inclusion of at least three-spin correlations.

Our calculations were based on the two five-spin clusters, shown in Fig. 2. Since we expect the dominant effects to come from the staggered-interaction mechanism, we considered only the leading terms in the Hamiltonian, as given by Eq. (7b), which have the advantage of a simple Ising form whose eigenstates can be written down by inspection. For the spins within each cluster, all of the interactions were treated exactly, while the interactions with spins outside the cluster were treated approximately using molecular fields. The field acting on the  $i$ th spin was taken to be

$$H_i = H_0 + \lambda_{1i}(M_+/M_0) + \lambda_{2i}(M_-/M_0) \quad (28)$$

where  $M_+$  and  $M_-$  are the magnetizations of the two sublattices determined self-consistently, and  $\lambda_{1i}$  and  $\lambda_{2i}$  are proportionality constants calculated by summing the interactions between the  $i$ th spin and its various neighbors, using the interaction constants given in Table I. Because of the inevitable errors inherent in any such cluster calculation, it was not deemed worthwhile to include the effects of the long-range dipolar interactions, and it was therefore not necessary to allow for the shape dependence, as in the earlier series expansion [Eq. (B4)].

A straightforward summation of the terms in the partition function leads to two coupled equations for  $M_+$  and  $M_-$  as a function of field and temperature, and these were solved numerically using a computer.

To test the accuracy of the approximation, we first estimated the Néel temperature. This was found to be 2.99 K in very reasonable agreement with the experimental value of 2.54 K. The model also reproduced correctly the first-order nature of the antiferromagnetic-paramagnetic phase transition at low temperatures (below about 1.5 K), as indicated by the expected Van der Waals loops in  $M$  and  $M_s$  as a function of field.

The model was then used to calculate the field dependence of the order parameter  $M_s$  at several temperatures, and in Fig. 5 we compare the experi-

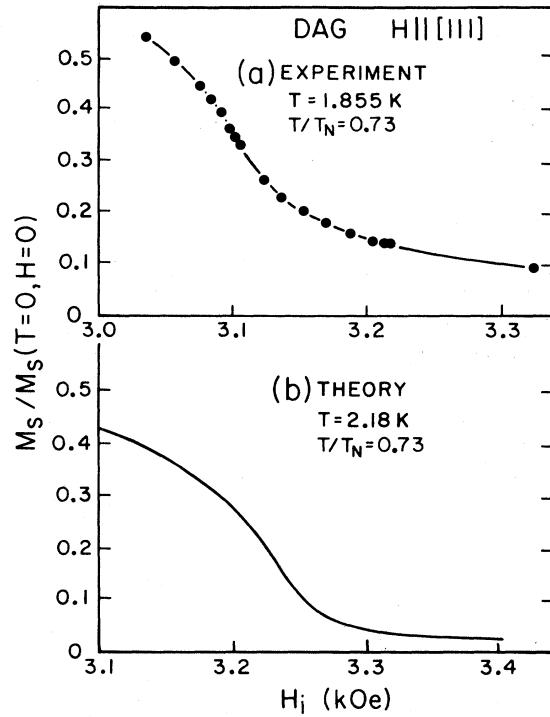


FIG. 5. Results for  $M_s$  as a function of  $H_i$  for DAG with  $H_i \parallel [111]$ . (a) Experimental results of Blume *et al.* (Ref. 6); (b) results of the cluster calculation for the same value of  $T/T_N$ .

mental results<sup>6</sup> at 1.855 K with the variation calculated for the same value of  $T/T_N$ .<sup>25</sup> It can be seen that several features of the experimental curve are well reproduced. Specifically, we may note (i) the value of  $M_s$  at the inflection, (ii) the width in field over which the pseudotransition occurs, and (iii) the magnitude of the "tail" of  $M_s$  in the high-field region.

In view of the simplicity of the model and the fact that it contains no adjustable parameters, we can regard the agreement between the calculation and experiment to be quite reasonable. Qualitatively similar results were found at other temperatures, and we can conclude that the staggered interaction mechanism can account for the effects observed in the neutron scattering experiments of Blume *et al.*<sup>6</sup> at temperatures between 1.7 and 2.5 K.

No detailed calculations were made using any of the other mechanisms, as represented by Eqs. (7c)–(7e), but there is little reason to believe that they would be significantly more effective in this region than at higher and lower temperatures. In the case of the  $g$ -value mechanism, this is confirmed by mean-field calculations carried out by Foglio and Blume,<sup>10</sup> who found that this mechanism is indeed far too weak to account for the observed neutron scattering results. In principle, it would not be too hard to include additional terms in the cluster calculation and for systems in which other mechanisms are important this might be a good approximation not only for intermediate temperatures, but also for higher and lower temperatures.

## VI. INDUCED STAGGERED FIELDS IN OTHER SYSTEMS

So far, we have concentrated primarily on one system, DAG, both because there have been a number of experimental observations of induced-staggered-field effects in DAG and because the microscopic structure and interactions in DAG are known rather precisely. However, it is clear from the symmetry arguments given by Alben *et al.*<sup>7</sup> that there must be many other systems in which such effects could be observed, and it is useful to consider what microscopic mechanisms might be important in some of these.

Apart from details such a lattice structure or the values of the various parameters, the Hamiltonian shown in Eq. (7) will apply to most other systems characterized by  $S' = \frac{1}{2}$  effective spins. The presence of specific terms in the Hamiltonian is, of course, dominated by symmetry considerations and, in particular cases, certain terms may be absent. In general, however, we may anticipate contributions to observable induced-staggered-field effects from all of the mechanisms which we have considered in this paper, the relative importance of each depending on the values of the individual parameters in the Hamiltonian.

In most systems the Ising-like terms [Eq. (7b)] will not be as dominant as they are in DAG, and we may therefore expect effects due to transverse  $g$  values [Eq. (7c)] and anisotropic non-Ising interactions [Eqs. (7d) and (7e)] to be more important. In the absence of detailed information it is not possible to make any general predictions, but it seems safe to anticipate quite complex situations. Since each of the induced-staggered-field mechanisms is associated with its own *sign* and temperature dependence, a wide variety of competing situations can be expected, and it would be of interest to look for some of these.

Among the systems which might show some of these effects are several of the rare-earth aluminum and gallium garnets. All of these are isostructural with DAG, and therefore of the appropriate symmetry to allow induced staggered fields. Electron-spin-resonance experiments have shown a wide variety of  $g$ -value anisotropies for the Kramers ions  $\text{Nd}^{3+}$ ,  $\text{Dy}^{3+}$ ,  $\text{Er}^{3+}$ , and  $\text{Yb}^{3+}$  in these garnets (see Wolf *et al.* in Ref. 15), and for at least the first three of these we would therefore expect large induced staggered fields from the  $g$ -value mechanism.

Thus, for example, for  $\text{Dy}^{3+}$  in yttrium gallium garnet [which should closely approximate to pure dysprosium gallium garnet (DGG)], we have (see Wolf *et al.* in Ref. 15 and see Ref. 26)  $g_x = 11.07$ ,  $g_y = 1.07$ , and  $g_z = 7.85$  and, substituting in Eq. (26), we find at high temperatures

$$\lim_{H \rightarrow \infty} \left| \frac{M_s}{M_{s0}} \right| = 0.267 \quad (29)$$

a value almost 700 times larger than that for DAG [Eq. (27)] and one which should be readily observable. Unfortunately, very little is known at this time about the other interactions in DGG, and it is therefore not possible to make any detailed predictions concerning the total effects which one might expect. However, it would seem quite likely that both the staggered-interactions mechanism and the non-Ising interactions will make significant contributions and it is possible that some of these effects will compete. A detailed study of this system, as well as other rare-earth gallium and aluminum garnets, would certainly be of interest.<sup>27</sup>

Another class of materials which have been predicted to show induced-staggered-field effects on the basis of symmetry,<sup>7</sup> are the transition-metal fluorides  $\text{MnF}_2$ ,  $\text{CoF}_2$ , and  $\text{FeF}_2$ . For  $\text{MnF}_2$  the effects may be expected to be extremely small, since  $\text{Mn}^{2+}$  is an  $S$ -state ion and both the  $g$  value and exchange interactions will therefore be highly isotropic, and similar for the two inequivalent ions in the unit cell. For  $\text{CoF}_2$ , on the other hand, we might expect significant contributions from both the  $g$ -value mechanism [Eq. (7c)] and non-Ising interactions [Eqs. (7d) and (7e)]. Unfortunately, there does not

appear to be enough information about the microscopic interactions in  $\text{CoF}_2$  to make detailed predictions, but we can estimate the contribution from the  $g$ -value effect using results of electron-spin-resonance experiments on  $\text{Co}^{2+}$  in  $\text{MgF}_2$ .<sup>28</sup> These experiments give  $g_x = 6.03$ ,  $g_y = 2.30$ , and  $g_z = 4.24$ , and, taking  $\Delta \sim 2k_B T_N \sim 76k_B$  and  $H = 20$  kOe, we find from Eq. (10) that at 4.2 K,

$$(\Delta M/M_0) \sim 9.7 \times 10^{-3}. \quad (30)$$

This is comparable with the effects calculated for DAG with a field eight times smaller (see Table II), but since the ordering temperature of  $\text{CoF}_2$  ( $T_N = 38$  K), is more than a factor 15 higher, it should be possible to use higher fields without inducing a phase transition. Comparable contributions may also be expected from anisotropic exchange interactions which will almost certainly reflect the low symmetry of the  $g$  values.

The symmetry of the rutile structure also allows a different kind of mechanism which has recently been studied by Radhakrishna *et al.*<sup>29</sup> Under the action of an appropriately oriented uniaxial stress, it is possible to distort the crystal in such a way that a term *linear* in an applied field can couple to the staggered magnetization, much as it does in a weak ferromagnet.<sup>30</sup> To interpret such a mechanism in terms of the microscopic spin Hamiltonian, one would need to estimate the strain dependence of the various interaction parameters, and this is beyond the scope of the present paper. However, we may note here that experiments on  $\text{CoF}_2$  by Radhakrishna *et al.*<sup>29</sup> did show measurable induced-staggered-field effects, and it seems clear that further study of this system would be of interest.

For  $\text{FeF}_2$  the situation is complicated by the fact that the  $S = 2$  ground state of the  $\text{Fe}^{2+}$  ions is split by the crystal field and spin-orbit coupling by about  $30 \text{ cm}^{-1}$ ,<sup>31</sup> which is comparable with the exchange interactions which lead to ordering at  $T_N \sim 80$  K.<sup>32</sup> The effective spin Hamiltonian will therefore include terms such as  $B_2^0 S_z^2$  and  $B_2^2 (S_x^2 - S_y^2)$  which will reflect the point symmetry at the  $\text{Fe}^{2+}$  sites. In particular, the difference between the two inequivalent sites will result in a change of sign of the term in  $B_2^2$  and this will lead to a difference in the moments at the two sites when a field is applied and hence to an induced staggered field. Since the  $g$  values and the coefficient  $B_2^2$  are all known, it is possible to estimate the size of the effect. A perturbation calculation similar to that performed for the  $g$ -value effect is straightforward, but since no experimental results are available we will simply estimate the order of magnitude of the effect. The perturbation has the form

$$V_5 = B_2^0 \sum_{i=a} [(S_i^x)^2 - (S_i^y)^2] - B_2^2 \sum_{i=b} [(S_i^x)^2 - (S_i^y)^2]. \quad (31)$$

Since we know from symmetry arguments<sup>7</sup> that the effect on the energy will be of order  $H^3$ , we will look for terms in a perturbation expansion of this order. Terms of this type can arise in two ways: (i) from the perturbation  $V_5$  in second order: This term will be of the form

$$\Delta E \approx |\langle 0 | V_5 | 2x \rangle|^2 / (E_0 - E_{2x}). \quad (32)$$

Since  $E_0 - E_{2x} \approx 2\Delta - 4\mu H$  and the matrix element is of order  $B_2^2$ , the resulting term of order  $H^3$  is obtained by expanding the denominator of Eq. (32) and is given approximately by

$$\Delta E \approx 4(B_2^2)^2 \mu^3 H^3 / \Delta^4; \quad (33)$$

(ii) From a third-order perturbation expansion involving  $V_5$  and  $V_1$  [Eq. (7c)]. This term is of order

$$\Delta E \approx \frac{\langle 0 | V_5 | 2x \rangle \langle 2x | V_1 | 1x \rangle \langle 1x | V_1 | 0 \rangle}{(E_0 - E_{2x})(E_0 - E_{1x})}. \quad (34)$$

Using the fact that the matrix element of  $V_1$  is of order  $g_x \mu_B H$  and that  $E_0 - E_{1x} \approx \Delta - 2\mu H$ , we can expand the denominators to obtain the  $H^3$  term. It is of order

$$\Delta E \approx 2B_2^2 \mu_B^2 g_x^2 \mu H^3 / \Delta^3. \quad (35)$$

The contributions of Eqs. (33) and (35) to the difference in the magnetizations of the two antiferromagnetic states are thus of order

$$\frac{\Delta M}{M_0} \sim \frac{6B_2^2 \mu_B^2 H^2}{\Delta^3} \left[ g_x^2 + O\left(\frac{B_2^2 g_z^2}{\Delta}\right) \right], \quad (36)$$

where we have written  $M_0 = N\mu \sim N\mu_B g_z$ . For  $\text{FeF}_2$ ,<sup>31,33</sup>  $B_2^2 \approx 1 \text{ cm}^{-1}$ ,  $g_z = 9.0$ ,  $g_x \approx g_y = 2.0$ , and taking  $\Delta \approx 2k_B T_N$  we find for  $H = 20$  kOe that the first term in Eq. (40) is  $2 \times 10^{-5}$  while the second is  $6 \times 10^{-6}$ . This is very small and probably negligible compared to the  $g$ -value effect, which itself will be quite small in this system. Contributions from the other mechanisms which we have considered will likewise be very small or zero (there are no staggered interactions in the rutile lattice), and it would appear that staggered-field effects may be difficult to observe in  $\text{FeF}_2$ . On the other hand, the high  $T_N$  and large anisotropy would make it possible to apply very large fields without inducing a phase transition and this could offset the smaller coefficients. Further study of this system would certainly be of interest.

It would seem clear that there is no shortage of microscopic mechanisms which can lead to induced staggered fields, although some effects may be very weak. As always, the first guide to potentially interesting systems must be the appropriate symmetry, and in this connection it is encouraging to note that

of the 59 compensated antiferromagnetic point groups, 38 allow coupling between the order parameter and applied fields in third or higher order.<sup>7</sup> Thus, a substantial number of known antiferromagnets should exhibit induced-staggered-field effects, with correspondingly wide varieties of strengths and temperature dependences.

## VII. CONCLUSION

In this paper we have considered a number of microscopic mechanisms which can contribute to induced-staggered-field effects. It is clear that there are several different contributions which can be important under different conditions and competition between different mechanisms is possible. Such competition can lead to relatively complex phase diagrams, in which the antiferromagnetic order parameter (staggered magnetization) changes sign one or more times as a function of temperature and field. Such phase diagrams may be of some interest in themselves, and they may also afford interesting opportunities for studying the dynamics of order-order transformations. In any case, one may expect a wide variety of observable induced-staggered-field effects in systems in which they are allowed by symmetry.<sup>7</sup>

Our detailed analysis for the particular case of dysprosium aluminum garnet has provided a quantitative explanation for the induced-staggered-field effects previously observed in optical<sup>5,9</sup> and neutron scattering experiments<sup>6</sup> and explained in qualitative terms by Blume *et al.*<sup>6</sup> We find that the dominant mechanism in the field and temperature region of interest arises from an unusual competition between ferromagnetic and antiferromagnetic Ising-like interactions. This suggests the possibility of further theoretical studies on induced-staggered-field effects in other Ising models with structures simpler than those of DAG, but with similar staggered interactions. One such model is the two-dimensional Kagomé lattice which we have studied previously (see Giordano and Wolf in Ref. 17 and see Ref. 18), but there are clearly other possibilities which may be of interest.

## ACKNOWLEDGMENTS

We would like to thank R. Alben, M. Blume, E-Yi Chen, J. F. Dillon, Jr., D. Mukamel, and M. F. Thorpe for a number of very useful discussions. One of us (W. P. W.) would also like to thank the Physics Department of Brookhaven National Laboratory for their hospitality which greatly facilitated the preparation of this manuscript. This work was supported in part by the National Science Foundation under Grant DMR 76-23102.

## APPENDIX A: CALCULATION OF THE $g$ -VALUE EFFECT

Here we calculate the  $g$ -value effect in DAG at low temperatures and low fields. First, we will determine the effect of the perturbation  $V_1$  [Eq. (7c)] on the ground state of the Hamiltonian  $\mathcal{H}_I$  [Eq. (7b)]. As discussed in the text, this yields the temperature-independent part of the  $g$ -value effect.

We will denote the ground state of the unperturbed Hamiltonian  $\mathcal{H}_I$  by  $|0\rangle$ .  $\mathcal{H}_I$  is just a simple Ising Hamiltonian, and  $|0\rangle$  is the product of the eigenstates of the operators  $S_i^z$ , with the eigenvalue of the  $S_i^z$  given by the spin direction in the antiferromagnetic ground state illustrated in Fig. 1. We will denote the excited states of  $\mathcal{H}_I$  in which one  $a$ - or one  $b$ -type spin is flipped from its ground-state value by  $|1x_i\rangle$  and  $|1y_i\rangle$ , respectively. Each of these states is  $(\frac{1}{2}N)$ -fold degenerate. The (unperturbed) energies of these states  $E_{1x}$  and  $E_{1y}$  are given by

$$\begin{aligned} E_{1x} &= E_0 + \Delta - 2\mu H, \\ E_{1y} &= E_0 + \Delta + 2\mu H, \end{aligned} \quad (A1)$$

where  $E_0$  is the unperturbed ground-state energy,  $\Delta$  is the  $H=0$  energy gap discussed in the text,  $\mu = \mu_B g_z / 2\sqrt{3}$ , and  $H$  is the magnitude of the field applied along the [111] direction. Note that for  $H > 0$  our calculation applies to the antiferromagnetic ground state in which the  $a$  spins are antiparallel to the field, which is the  $A^+$  state.

The shift in the ground-state energy to second order in  $V_1$  is

$$\Delta E_0 = \sum_{i=a} \frac{|\langle 0|V_1|1x_i\rangle|^2}{E_0 - E_{1x}} + \sum_{i=b} \frac{|\langle 0|V_1|1y_i\rangle|^2}{E_0 - E_{1y}}. \quad (A2)$$

Inserting Eqs. (A1) and (7c) into Eq. (A2) gives

$$\Delta E_0 = \frac{1}{12} N \mu_B^2 H^2 \left( \frac{g_x^2}{\Delta - 2\mu H} + \frac{g_y^2}{\Delta + 2\mu H} \right), \quad (A3)$$

where  $N$  is the total number of spins. Expanding the denominators in Eq. (A3) gives Eq. (8) in the text.

Next we calculate the temperature dependence of the  $g$ -value effect at low temperatures. To do this we need to compute the effect of  $V_1$  on the lowest-lying excited states of  $H_I$ ,  $|1x\rangle$  and  $|1y\rangle$ . This in turn requires that we consider the states with two  $a$  spins flipped from the ground-state configuration,  $|2x_{ij}\rangle$ , two  $b$  spins flipped,  $|2y_{ij}\rangle$ , and  $a$  and one  $b$  spin flipped,  $|1x_i, 1y_j\rangle$ . The energies of these states are given approximately by

$$\begin{aligned} E_{2x} &= E_0 + 2\Delta - 4\mu H, \\ E_{2y} &= E_0 + 2\Delta + 4\mu H, \\ E_{1x,1y} &= E_0 + 2\Delta. \end{aligned} \quad (A4)$$

Equation (A4) is only approximate because we have neglected the effects of correlations — that is, if the two spins which are flipped are near neighbors, then the  $H=0$  excitation energy will not be twice the energy required to flip one isolated spin, since the two spins interact. We note however, that in DAG (A4) is in error by only 10% (at  $H=0$ ) when the spins are nearest neighbors, and by much less if they are more widely separated. This level of accuracy is more than adequate for our purposes, since, in the range of temperatures and fields with which we are concerned, the temperature-dependent part of the  $g$ -value effect will turn out to be much smaller than the temperature-independent part.

$$\Delta E_{1x} = \frac{1}{6} \mu_B^2 H^2 \left\{ \left[ -\frac{1}{2} N \left( \frac{g_x^2}{\Delta - 2\mu H} + \frac{g_y^2}{\Delta + 2\mu H} \right) \right] + \frac{2g_x^2}{\Delta - 2\mu H} \right\} \quad (\text{A6})$$

Comparing Eq. (A6) with Eq. (A3) we see that the term in square brackets is equal to the shift of the ground-state energy, so that the change in  $(E_{1x} - E_0)$  due to the perturbation is just

$$\Delta' E_{1x} = \frac{1}{3} \mu_B^2 H^2 [g_x^2 / (\Delta - 2\mu H)] \quad (\text{A7})$$

The total energy difference is then  $\Delta' E_{1x} + \Delta - 2\mu H$  or

$$\begin{aligned} \Delta_x &= \Delta - 2\mu H + \frac{1}{3} \mu_B^2 H^2 [g_x^2 / (\Delta - 2\mu H)] \quad (\text{A8a}) \\ &\approx \Delta - \mu_B g_z H / \sqrt{3} + (g_x^2 \mu_B^2 H^2 / 3\Delta) (1 + \mu_B g_z H / \sqrt{3}\Delta) \quad (\text{A8b}) \end{aligned}$$

where we have substituted  $\mu = g_z \mu_B / 2\sqrt{3}$ . A similar calculation for the state  $|1y\rangle$  gives

$$\begin{aligned} \Delta_y &= \Delta + 2\mu H + \frac{1}{3} \mu_B^2 H^2 [g_y^2 / (\Delta + 2\mu H)] \quad (\text{A9a}) \\ &\approx \Delta + g_z \mu_B H / \sqrt{3} + (g_y^2 \mu_B^2 H^2 / 3\Delta) (1 - \mu_B g_z H / \sqrt{3}\Delta) \quad (\text{A9b}) \end{aligned}$$

The partition function is then

$$\begin{aligned} Z &= \exp(-E_g / k_B T) \left[ 1 + \frac{1}{2} N \exp(-\Delta_x / k_B T) \right. \\ &\quad \left. + \frac{1}{2} N \exp(-\Delta_y / k_B T) + \dots \right] \quad (\text{A10}) \end{aligned}$$

where  $E_g = E_0 + \Delta E_0$  is the energy of the ground state to second order [Eq. (A3)], and the terms that have been dropped correspond to higher-lying excited states such as  $|2x\rangle$ , which can be neglected at low temperatures compared to the terms corresponding to  $|1x\rangle$  and  $|1y\rangle$ . From Eq. (A10) the free energy is

To second order, the effect of  $V_1$  on the energy of  $|1x\rangle$  is given by

$$\begin{aligned} \Delta E_{1x} &= \frac{|\langle 1x_i | V_1 | 0 \rangle|^2}{E_{1x} - E_0} \\ &\quad + \sum_{j=b} \frac{|\langle 1x_i | V_1 | 1x_j, 1y_j \rangle|^2}{E_{1x} - E_{1x,1y}} \\ &\quad + \sum_{j=a} \frac{|\langle 1x_i | V_1 | 2x_{ij} \rangle|^2}{E_{1x} - E_{2x}} \quad (\text{A5}) \end{aligned}$$

Inserting Eqs. (A1), (A4), and (7c) into (A5) gives after a little rearranging

finally

$$\begin{aligned} F &= -k_B T \ln Z \\ &= E_g - \frac{1}{2} N k_B T \\ &\quad \times [\exp(-\Delta_x / k_B T) + \exp(-\Delta_y / k_B T)] \quad (\text{A11}) \end{aligned}$$

which is the expression given in Eq. (9).

#### APPENDIX B: CALCULATION OF THE STAGGERED-INTERACTION EFFECT

Here we calculate the leading terms in the low-temperature series expansion for the two sublattice magnetizations  $M_{\pm}$  for DAG, using only the Ising-like terms given in Eq. (7b). Since the interaction parameters  $K_{ij}$  are both positive and negative, this gives an estimate of the effect of the staggered-interaction mechanism discussed qualitatively in Sec. III B.

Starting from the ground state  $A^+$ , various excitations involving one, two, and three spin reversals were considered for inclusion in the series. These are shown diagrammatically in Table IV which also gives the corresponding excitation energies and degeneracies. A number of other excitations involving reversals of three spins shown in Table V were also considered, but were not included in the calculation since these make only very small contributions to the series. [The terms which were omitted (Table V) were each less than 1% of the largest term in the temperature and field range of interest.]

Given the energies and degeneracies of the excitations, the partition function  $Z$  can be written by inspection. We define  $A = \exp(-4K_1 / k_B T)$ ,  $B = \exp(-4K_2 / k_B T)$ , and  $C_{\pm} = (-2\mu H_{\pm} / k_B T)$ ,



TABLE IV. Excitations corresponding to reversals of one, two, and three spins from the  $A^+$  ground state.  $\oplus$  and  $\ominus$  denote reversals of  $b$ - and  $a$ -type spins, respectively. The solid and dashed lines indicate that the spins are first or second neighbors, respectively. If there is no connecting line, the spins are more distant neighbors. Note that only those spin excitations which were included in the calculation of induced-staggered-field effects are shown here. The three-spin excitations which were not used in the series expansion are given in Table V.

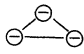
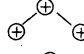

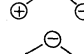
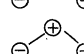
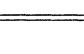
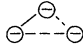
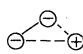
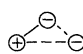
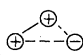
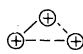
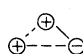
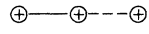
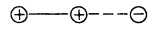
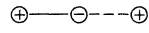
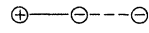
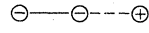
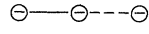



Excitation	Energy	Degeneracy
$\oplus$	$8K_1 + 16K_2 + 2\mu H_+$	$\frac{1}{2}N$
$\ominus$	$8K_1 + 16K_2 - 2\mu H_-$	$\frac{1}{2}N$
$\oplus\text{---}\oplus$	$12K_1 + 32K_2 + 4\mu H_+$	$\frac{1}{2}N$
$\oplus\text{---}\ominus$	$12K_1 + 32K_2 + 2\mu H_+ - 2\mu H_-$	$N$
$\ominus\text{---}\ominus$	$12K_1 + 32K_2 - 4\mu H_-$	$\frac{1}{2}N$
$\oplus\text{---}\oplus$	$16K_1 + 28K_2 + 4\mu H_+$	$N$
$\oplus\text{---}\ominus$	$16K_1 + 28K_2 + 2\mu H_+ - 2\mu H_-$	$2N$
$\ominus\text{---}\ominus$	$16K_1 + 28K_2 - 4\mu H_-$	$N$
$\oplus\oplus$	$16K_1 + 32K_2 + 4\mu H_+$	$\frac{1}{4}N(\frac{1}{2}N - 7)$
$\oplus\ominus$	$16K_1 + 32K_2 + 2\mu H_+ - 2\mu H_-$	$\frac{1}{2}N(\frac{1}{2}N - 6)$
$\ominus\ominus$	$16K_1 + 32K_2 - 4\mu H_-$	$\frac{1}{4}N(\frac{1}{2}N - 7)$
	$12K_1 + 48K_2 - 6\mu H_-$	$\frac{1}{6}N$
	$16K_1 + 48K_2 + 6\mu H_+$	$\frac{1}{2}N$
	$12K_1 + 48K_2 + 4\mu H_+ - 2\mu H_-$	$\frac{1}{2}N$
	$16K_1 + 48K_2 + 4\mu H_+ - 2\mu H_-$	$N$
	$16K_1 + 48K_2 + 2\mu H_+ - 4\mu H_-$	$2N$
	$16K_1 + 48K_2 + 2\mu H_+ - 4\mu H_-$	$\frac{1}{2}N$

TABLE V. Three-spin excitations from the  $A^+$  ground state which were not included in the series expansion [Eq. (11)]. See Table IV for an explanation of the notation.

	$\ominus$	$\ominus$	$\ominus$
	$\oplus$	$\oplus$	$\oplus$
	$\oplus$	$\oplus$	$\ominus$
	$\oplus$	$\ominus$	$\oplus$
	$\oplus$	$\ominus$	$\ominus$
	$\ominus$	$\ominus$	$\oplus$
	$\ominus$	$\ominus$	$\ominus$
	$\oplus$	$\text{---}$	$\oplus$
	$\oplus$	$\text{---}$	$\oplus$
	$\oplus$	$\text{---}$	$\oplus$
	$\oplus$	$\text{---}$	$\oplus$
	$\ominus$	$\text{---}$	$\oplus$
	$\oplus$	$\oplus$	$\oplus$
	$\oplus$	$\oplus$	$\ominus$
	$\oplus$	$\ominus$	$\ominus$

where  $\mu = \mu_B g_z / 2\sqrt{3}$  and  $H_{\pm}$  is the field (molecular fields included) on the sublattices parallel and antiparallel to the [111] direction. Including the 17 excitations shown in Table V then gives

$$\begin{aligned}
Z = \exp[-(N\mu/2k_B T)(H_- - H_+)] & [1 + \frac{1}{2}NA^2B^4(C_+ + C_-^{-1}) + (\frac{1}{2}N)A^3B^8(C_+^2 + C_-^{-2}) + NA^4B^7(C_+^2 + C_-^{-2}) \\
& + NA^3B^8C_+C_-^{-1} + 2NA^4B^7C_+C_-^{-1} + (\frac{1}{2}N)(\frac{1}{2}N - 6)A^4B^8C_+C_-^{-1} \\
& + (\frac{1}{4}N)(\frac{1}{2}N - 7)A^4B^8(C_+^2 + C_-^{-2}) + (\frac{1}{6}N)A^3B^{12}C_-^{-3} + (\frac{1}{2}N)A^4B^{12}C_+^3 \\
& + (\frac{1}{2}N)A^3B^{12}C_+^2C_-^{-1} + NA^4B^{12}C_+^2C_-^{-1} + 2NA^4B^{12}C_+C_-^{-2} + (\frac{1}{2}N)A^4B^{12}C_+C_-^{-2}] ,
\end{aligned} \tag{B1}$$

where  $N$  is again the total number of spins. From Eq. (B1) we can derive the free energy

$$\begin{aligned}
F = -k_B T \ln Z = \frac{1}{2}N\mu(H_- - H_+) - Nk_B T & [\frac{1}{2}A^2B^4(C_+ + C_-^{-1}) + \frac{1}{2}A^3B^8(C_+^2 + C_-^{-2}) + A^4B^7(C_+^2 + C_-^{-2}) + A^3B^8C_+C_-^{-1} \\
& + 2A^4B^7C_+C_-^{-1} - 3A^4B^8C_+C_-^{-1} - \frac{7}{4}A^4B^8(C_+^2 + C_-^{-2}) \\
& + \frac{1}{6}A^3B^{12}C_-^{-3} + \frac{1}{2}A^4B^{12}C_+^3 + \frac{1}{2}A^3B^{12}C_+^2C_-^{-1} \\
& + A^4B^{12}C_+^2C_-^{-1} + \frac{5}{2}A^4B^{12}C_+C_-^{-2}] .
\end{aligned} \tag{B2}$$

As usual, the terms proportional to  $N^2$ ,  $N^3$ , etc., cancel in the expansion of the logarithm, leaving  $F$  proportional to  $N$ . The corresponding magnetizations of the two sublattices in the direction of the applied field are given by

$$M_+ = -\frac{\partial F}{\partial H_+} = N\mu \left( \frac{1}{2} - A^2 B^4 C_+ - 2A^3 B^8 C_+^2 - 4A^4 B^7 C_+^2 - 2A^3 B^8 C_+ C_-^{-1} - 4A^4 B^7 C_+ C_-^{-1} \right. \\ \left. + 6A^4 B^8 C_+ C_-^{-1} + 7A^4 B^8 C_+^2 - 3A^4 B^{12} C_+^3 - 2A^3 B^{12} C_+^2 C_-^{-1} \right. \\ \left. - 4A^4 B^{12} C_+^2 C_-^{-1} - 5A^4 B^{12} C_-^{-2} C_+ \right), \quad (\text{B3a})$$

$$M_- = N\mu \left( -\frac{1}{2} + A^2 B^4 C_-^{-1} + 2A^3 B^8 C_-^{-2} + 4A^4 B^7 C_-^{-2} + 2A^3 B^8 C_+ C_-^{-1} + 4A^4 B^7 C_+ C_-^{-1} - 6A^4 B^8 C_+ C_-^{-1} \right. \\ \left. - 7A^4 B^8 C_-^{-2} + A^3 B^{12} C_-^{-3} + A^3 B^{12} C_+^2 C_-^{-1} + 2A^4 B^{12} C_+^2 C_-^{-1} + 10A^4 B^{12} C_+ C_-^{-2} \right). \quad (\text{B3b})$$

The mean fields  $H_{\pm}$  may be written

$$H_+ = H_0 + \lambda_1 (M_-/M_0) + \lambda_2 (M_+/M_0), \quad (\text{B4a})$$

$$H_- = H_0 + \lambda_1 (M_+/M_0) + \lambda_2 (M_-/M_0), \quad (\text{B4b})$$

where  $H_0$  is the applied field,  $\lambda_1$  and  $\lambda_2$  are the inter-sublattice and intrasublattice coupling constants, respectively, and  $M_0$  is the saturation magnetization  $N\mu$ . The constants  $\lambda_1$  and  $\lambda_2$  are simply lattice sums which can be calculated from the  $g$  tensor, lattice spacings, and the value of  $K_3$ , the third-nearest-neighbor-interaction parameter. Since the sum of magnetic-dipole interactions is shape dependent we must specify a particular sample shape for the param-

eters  $\lambda_1$  and  $\lambda_2$ . We shall here choose a long needle with zero demagnetizing factor, since the experimental results had previously been corrected to this shape. The values obtained for this case are<sup>34</sup>

$$\lambda_1^{\infty} = 4640 \text{ Oe}, \quad \lambda_2^{\infty} = 1310 \text{ Oe}, \quad (\text{B5})$$

where we had added the superscript  $\infty$  to emphasize that the values apply to a long needle sample.

Combining Eqs. (B3a) and (B3b) with Eqs. (B4a) and (B4b) gives two coupled equations in  $M_+$  and  $M_-$  which can be solved numerically to yield  $M = M_+ + M_-$  as a function of field and temperature. The results are shown in Fig. 3, together with the experimental results of Dillon *et al.*<sup>9</sup>

\*Present address: Phys. Dept. Purdue Univ., West Lafayette, Ind. 47907.

<sup>1</sup>D. P. Landau, B. E. Keen, B. Schneider, and W. P. Wolf, Phys. Rev. B **3**, 2310 (1971).

<sup>2</sup>W. P. Wolf, in *Proceedings of the 20th Conference on Magnetism and Magnetic Materials, San Francisco, 1974*, edited by C. D. Graham, Jr., G. H. Lander, and J. J. Rhyne, AIP Conf. Proc. No. 24 (AIP, New York, 1975), p. 255.

<sup>3</sup>References 1 and 2 also contain extensive references to earlier work on DAG.

<sup>4</sup>W. P. Wolf, B. Schneider, D. P. Landau, and B. E. Keen, Phys. Rev. B **5**, 4472 (1972).

<sup>5</sup>J. F. Dillon, Jr., E. Yi Chen, and W. P. Wolf, in *Proceedings of the International Conference on Magnetism, Moscow*, (Nauka, Moscow, 1974), Vol. 6, p. 38.

<sup>6</sup>M. Blume, L. M. Corliss, J. M. Hastings, and E. Schiller, Phys. Rev. Lett. **32**, 544 (1974).

<sup>7</sup>R. Alben, M. Blume, L. M. Corliss, and J. M. Hastings, Phys. Rev. B **11**, 295 (1975).

<sup>8</sup>The concept of a real staggered field which couples to the order parameter was first introduced by R. B. Griffiths [Phys. Rev. Lett. **24**, 715 (1970)], and it is now used widely in discussions of the phase diagrams of antiferromagnets. More recently, Sarbach and Fisher [S. Sarbach and M. E. Fisher, J. Appl. Phys. **49**, 1350 (1978); M. E. Fisher and S. Sarbach, Phys. Rev. Lett. **41**, 1127 (1978)] have pointed out that it may be necessary to con-

sider a second kind of field  $h_3$ , which appears in the free-energy expansion. This field also couples to the order parameter, although as noted by Sarbach and Fisher its physical interpretation is not immediately obvious. For the purpose of the present paper it is not necessary to distinguish between these fields since the only fields which are actually applied are the components of the uniform field. The observable effects all result from terms in the microscopic-interaction Hamiltonian which lead to features which resemble those which would result from the application of a staggered field. We will therefore follow the convention of referring to these as "induced-staggered-field effects."

<sup>9</sup>J. F. Dillon, Jr., E. Yi Chen, N. Giordano, and W. P. Wolf, Phys. Rev. Lett. **33**, 98 (1974).

<sup>10</sup>M. E. Foglio and M. Blume, Phys. Rev. B **15**, 3465 (1977).

<sup>11</sup>M. Ball, M. T. Hutchings, M. J. M. Leask, and W. P. Wolf, in *Proceedings of the Eighth International Congress on Low Temperature Physics*, edited by R. O. Davies (Butterworths, London, 1963), p. 248.

<sup>12</sup>A. Herpin and P. Mériel, C. R. Acad. Sci. Paris **259**, 2416 (1964).

<sup>13</sup>J. M. Hastings, L. M. Corliss, and C. G. Windsor, Phys. Rev. **138**, A176 (1965).

<sup>14</sup>W. P. Wolf, *Proceedings of the International Conference on Magnetism, Nottingham, 1964* (Institute of Physics and Physical Society, London, 1964), p. 555.

- <sup>15</sup>We have deviated from the earlier convention [see for example W. P. Wolf, M. Ball, M. T. Hutchings, M. J. M. Leask, and A. F. G. Wyatt, *J. Phys. Soc. Jpn.* **17**, 443 (1962)] in which  $g_x$  was arbitrarily defined as the larger of the two  $g$  values perpendicular to  $g_z$ . In practice it is very difficult to relate these two  $g$  values with specific lattice sites, as we have done here, but it is a distinction which is important in principle, as we shall see in this paper. To distinguish  $g_x$  and  $g_y$  experimentally by means of a direct measurement, one might use electron nuclear double resonance (ENDOR) to relate the  $Dy^{3+}$  spin to the surrounding  $O^{2-}$  or  $Al^{3+}$  sites and hence to the crystal axes.
- <sup>16</sup>J. L. Lewis, thesis (Yale University, 1971) (unpublished).
- <sup>17</sup>The competing nature of ferromagnetic and antiferromagnetic interactions in DAG has been recognized previously (see for example, Ref. 4), and it was cited as the cause for the smallness of the Curie-Weiss  $\theta$ , which reflects the sum of all the interactions. However, the significance of the topological arrangement of interactions with competing signs was not recognized until recently [see N. Giordano and W. P. Wolf, in *Proceedings of the 20th Conference on Magnetism and Magnetic Materials, San Francisco, 1974*, edited by C. D. Graham, Jr., G. H. Lander, and J. J. Rhyne, AIP Conf. Proc. No. 24 (AIP, New York, 1975), p. 333].
- <sup>18</sup>N. Giordano, thesis (Yale University, 1977) (unpublished).
- <sup>19</sup>B. Schneider, D. P. Landau, B. E. Keen, and W. P. Wolf, *Phys. Lett.* **23**, 210 (1966).
- <sup>20</sup>A more detailed analysis [D. P. Landau, thesis (Yale University, 1967) (unpublished)] has shown that there is, in fact, a nondipolar contribution also to the fourth-nearest-neighbor interaction, but this is quite small and may be neglected in the present discussion.
- <sup>21</sup>D. Mukamel and M. Blume, *Phys. Rev. B* **15**, 4516 (1977).
- <sup>22</sup>There is a misprint in Eq. (8) of Ref. 21, in that there is a factor  $\alpha$  missing for all of the terms under the summation signs. [M. Blume (private communication).]
- <sup>23</sup>J. F. Dillon, Jr. and E. Yi Chen (private communication).
- <sup>24</sup>J. H. Van Vleck, *J. Chem. Phys.* **5**, 320 (1937).
- <sup>25</sup>It would clearly be misleading to compare the experimental results with a calculation at the same temperature, since it is already established that the model gives a somewhat higher value for  $T_N$ . By using the same *reduced* temperature  $T/T_N$ , much of this discrepancy should be removed.
- <sup>26</sup>As noted previously, simple electron-spin-resonance experiments cannot distinguish between  $g_x$  and  $g_y$ . Interchanging the assignment of the observed  $g$  values will simply reverse the sign of the induced staggered magnetization.
- <sup>27</sup>A neutron scattering study of DGG is currently under way [M. Steiner, L. M. Corliss, J. M. Hastings, M. Blume, N. Giordano, and W. P. Wolf, in the Proceedings of the International Conference on Magnetism, Munich, 1979 (unpublished)] and the preliminary results which have been obtained for  $T \gg T_N$  are in good agreement with the theoretical predictions based on Eq. (22).
- <sup>28</sup>H. M. Gladney, *Phys. Rev.* **143**, 198 (1966).
- <sup>29</sup>P. Radhakrishna, P. J. Brown, D. Herrmann-Ronzaud, and R. Alben, *J. Phys. C* **11**, 2851 (1978).
- <sup>30</sup>I. E. Dzialoshinskii, *Zh. Eksp. Teor. Fiz.* **32**, 1547 (1957); [*Sov. Phys. JETP* **5**, 1259 (1957)].
- <sup>31</sup>M. Tinkham, *Proc. Phys. Soc. (London)* **68**, 258 (1955).
- <sup>32</sup>See, for example, R. A. Erickson, *Phys. Rev.* **90**, 779 (1953).
- <sup>33</sup>M. Tinkham, *Proc. R. Soc. (London) Ser. A* **236**, 535 (1956).
- <sup>34</sup>In practice, it was convenient to estimate the  $\lambda$ 's from two experimentally determined parameters which are related to the sums of interactions. The energy  $\Delta$  required to reverse on spin at  $T=0$ ,  $H=0$ , is given by  $\Delta = 8|K_1| + 16|K_2| + (-\lambda_1 + \lambda_2)\mu$ , while the Curie-Weiss  $\theta$  is given by  $\theta = (\mu/2k_B)(\lambda_1 + \lambda_2)$ . Using the values  $\theta = \theta_{\text{sphere}} + \frac{4}{3}\pi\lambda_v = 1.04$  K (here  $\theta_{\text{sphere}}$  is the Curie-Weiss  $\theta$  for a sphere and  $\lambda_v$  is the Curie constant) and  $\mu = \mu_B g_z / 2\sqrt{3} = 4.82 \times 10^{-20}$  erg/Oe given in Ref. 4, together with the values of  $K_1$ ,  $K_2$ , and  $\Delta$  given in Table I, we find the values for  $\lambda_1$  and  $\lambda_2$  given in the text.